

Magnetotransport properties of noble metals containing rare-earth impurities.

I. Quadrupole scattering by rare-earth impurities in gold*

A. Fert, R. Asomoza, D. H. Sanchez,[†] and D. Spanjaard

Laboratoire de Physique des Solides,[‡] Université de Paris-Sud, 91405 Orsay, France

A. Friederich

Laboratoire Central de Recherche Thomson, 91401 Orsay, France

(Received 16 March 1977)

We report measurements of the magnetoresistance of gold containing rare-earth impurities in longitudinal and transverse magnetic fields. For rare-earths with orbital magnetism the dominant effect is an anisotropic magnetoresistance due to the scattering of the conduction electrons by the electric quadrupole moment of the $4f$ shell. This effect vanishes for gadolinium impurities (no quadrupole moment). We present a model of the anisotropic magnetoresistance induced by quadrupole scattering. From the analysis of the experimental results we derive the strength of the interaction of the conduction electrons with the quadrupole moment of the $4f$ shell.

I. INTRODUCTION

Magnetoresistance measurements¹ have shown that the resistivity cross section of rare-earth (RE) impurities in gold or silver is anisotropic, i.e., different according to whether the current is parallel or perpendicular to the magnetic moment of the rare earth. The resistivity anisotropy vanishes for gadolinium impurities and changes its sign at the middle of the series of the heavy rare earths, between Ho and Er, which shows that the resistivity anisotropy is due to aspherical Coulomb scattering and mostly to quadrupole scattering.¹ Similar results have been recently found in other magnetic alloys.^{2,3}

We present in this paper more extended series of magnetoresistance measurements on gold containing RE impurities (Sec. II) together with a model of the scattering by the $4f$ quadrupole (Sec. III). The resistivity anisotropy induced by quadrupole scattering is shown to be proportional to $[\langle\langle J_z^2 \rangle\rangle - \frac{1}{3}J(J+1)]$, where $\langle\langle J_z^2 \rangle\rangle$ is the mean value of the square of the component of the $4f$ moment in the field direction. This accounts for the very different field and temperature dependences of the resistivity anisotropy which are observed when the ground state in the crystal field is a triplet (or quartet), a Kramers doublet, or a singlet, respectively (Sec. IV). In Sec. V, we concentrate on the Au:Ho alloys. After an analysis of the crystal-field effects, we derive from the experimental data the *interaction of the conduction electrons with the $4f$ quadrupole*. We find that this interaction is nearly as large as the exchange interaction. The importance of the quadrupole interaction for RE ions has been recently suggested by several theoretical⁴ or experimental⁵ works. Our experiments provide interesting data on this interaction.

II. EXPERIMENTAL RESULTS

We have measured the magnetoresistance of gold containing heavy RE impurities at lower concentrations than 1 at.%. The measurements were performed in longitudinal and transverse magnetic field up to 40 kG and between 1.2 and 36 K. The preparation of the specimens (polycrystalline foils) and the experimental setup have already been described.⁶

Figures 1–5 show the main features of the observed effects. For gold with gadolinium impurities (no quadrupole) Fig. 1 exhibits a negative magnetoresistance which is obviously linked to the magnetization of the impurities (it vanishes at high temperature) and which is isotropic, i.e., independent of the angle between the field and the current. This is the usual negative isotropic magnetoresistance of the dilute magnetic alloys which is due to exchange scattering.^{7,8} The magnetoresistance

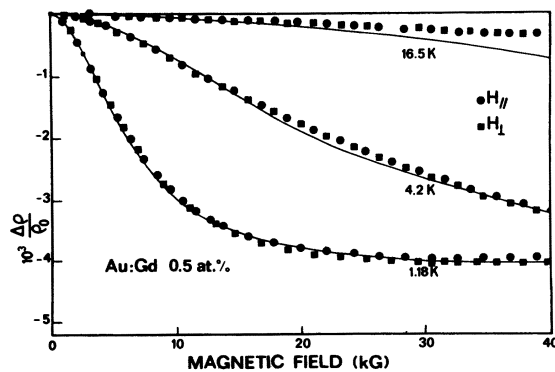


FIG. 1. Magnetoresistance of a 0.5-at. % Au:Gd alloy in transverse and longitudinal magnetic fields at several temperatures. The solid lines correspond to $\Delta\rho/\rho_0 = -3.98 \times 10^{-3} [B_{7/2} (g\mu_B H/k_B T)]^2$.

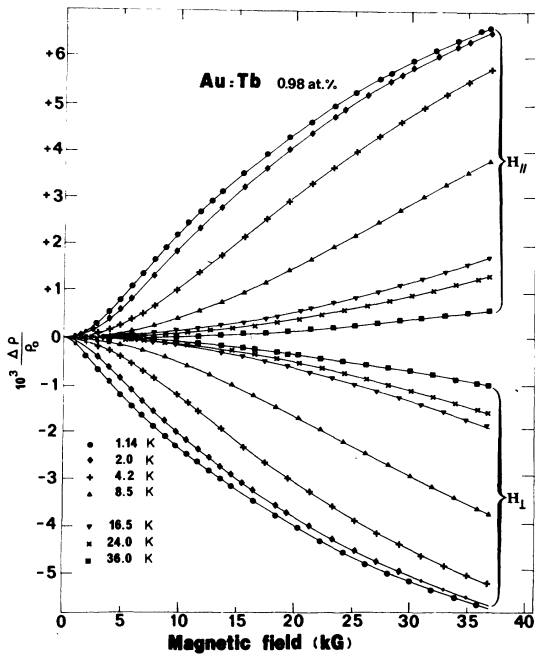


FIG. 2. Magnetoresistance of a 0.98-at. % Au:Tb alloy in transverse and longitudinal fields at several temperatures.

observed for impurities with orbital momentum (Figs. 2-5) is quite different: the magnetoresistance is linked to the impurity magnetization again but now longitudinal and transverse magnetoresis-

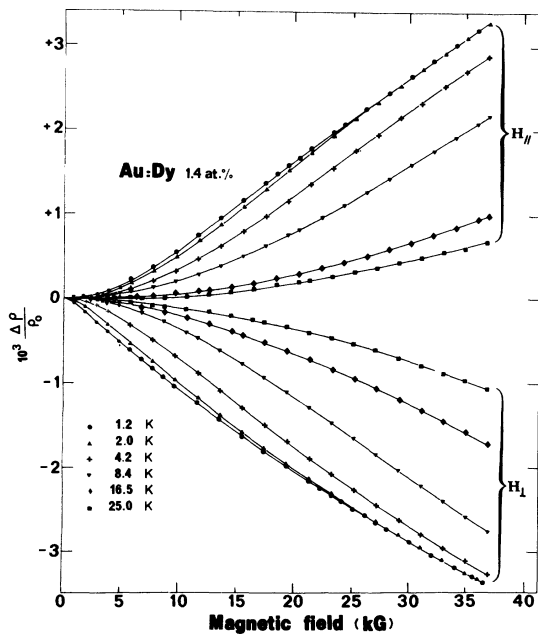


FIG. 3. Magnetoresistance of a 1.4-at. % Au:Dy alloy in transverse and longitudinal fields at several temperatures.

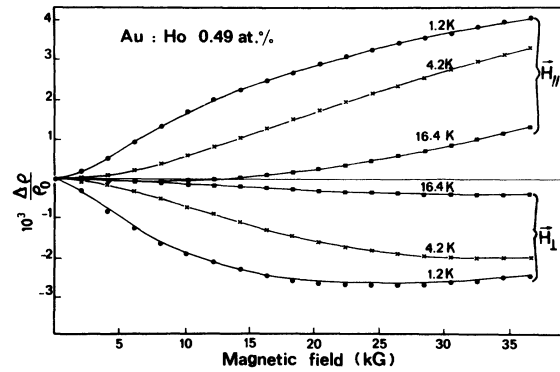


FIG. 4. Magnetoresistance of a 0.49-at. % Au:Ho alloy in transverse and longitudinal fields at several temperatures.

tance have opposite signs. Such an anisotropic magnetoresistance is the dominant effect when a $4f$ quadrupole exists. The resistivity anisotropy $(\rho_{||} - \rho_{\perp})/\rho_0$ is positive for Tb, Dy, and Ho and negative for Er, Tm, and Yb.

The resistivity of a polycrystal is written as

$$\rho(H) = \rho_0 + \Delta\rho_l(H) + (\cos^2\theta - \frac{1}{3})\Delta\rho_A(H), \quad (1)$$

where H is the magnitude of the magnetic field, θ is the angle between the field and the current, and ρ_0 is the resistivity at zero field. We shall see that, in the model presented in Sec. III, the quadrupole scattering contributes to the anisotropic part of the magnetoresistance, i.e., to $\Delta\rho_A(H)$, and that the exchange scattering contributes to the

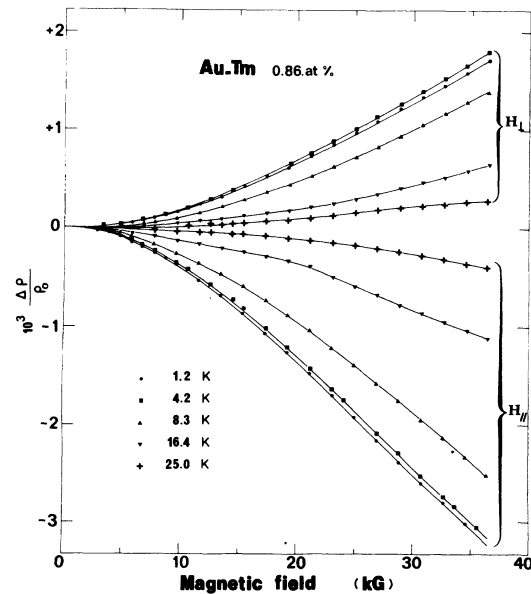


FIG. 5. Magnetoresistance of a 0.86-at. % Au:Tm alloy in transverse and longitudinal fields at several temperatures.

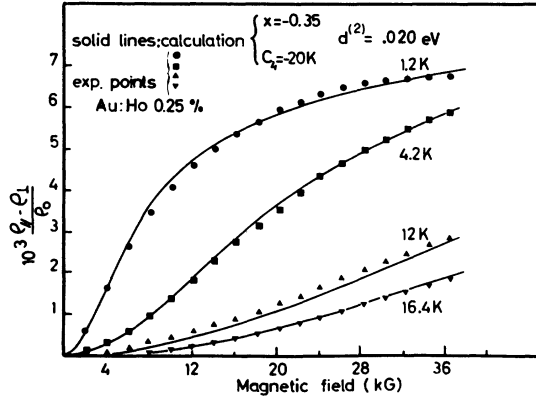


FIG. 6. Resistivity anisotropy $(\rho_{\parallel} - \rho_{\perp})/\rho_0$ of a 0.25-at. % Au:Ho alloy versus magnetic field at several temperatures: experimental points (after a small correction to eliminate the normal magnetoresistance) and calculated curves (for $x = -0.35$, $C_4 = -20$ K, $d^{(2)} = 0.20$ eV).

isotropic part, i.e., to $\Delta\rho_I(H)$. $\Delta\rho_A(H)$ and $\Delta\rho_I(H)$ can be extracted from the experimental results by the following obvious expressions:

$$\Delta\rho_A(H) = \rho_{\parallel}(H) - \rho_{\perp}(H), \quad (2)$$

$$\Delta\rho_I(H) = \frac{1}{3}[\rho_{\parallel}(H) - \rho_0] + \frac{2}{3}[\rho_{\perp}(H) - \rho_0], \quad (3)$$

where $\rho_{\parallel}(H)$ and $\rho_{\perp}(H)$ are the resistivities in longitudinal and transverse fields. We have plotted in Figs. 6–8 and 10 the resistivity anisotropy $(\rho_{\parallel} - \rho_{\perp})/\rho_0$ for Au:Ho, Au:Er, and Au:Tm alloys, and in Fig. 9, the isotropic part of the magnetoresistance $[(\rho_{\parallel} - \rho_0) + 2(\rho_{\perp} - \rho_0)]/3\rho_0$ for a Au:Ho alloy. Figures 6, 9, and 10 for Au:Ho alloys represent only the magnetoresistance due to the magnetic impurities after subtraction from the experimental curves of the normal magnetoresistance. The anisotropic and isotropic normal contributions have been found from the Kohler functions of the normal

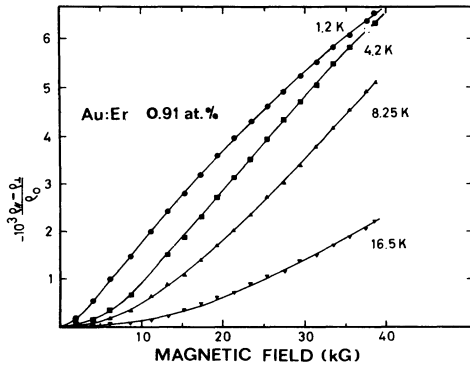


FIG. 7. Resistivity anisotropy $(\rho_{\parallel} - \rho_{\perp})/\rho_0$ of a 0.91-at. % Au:Er alloy versus magnetic field at several temperatures (raw experimental points; the solid lines are to guide the eye).

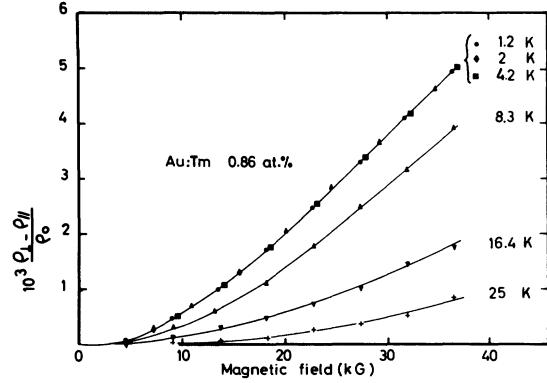


FIG. 8. Resistivity anisotropy $(\rho_{\parallel} - \rho_{\perp})/\rho_0$ of 0.86-at. % Au:Tm alloy versus magnetic field at several temperatures (raw experimental points; the solid lines are to guide the eye).

magnetoresistance (determined on nonmagnetic alloys) and represent only small corrections (for example, in Fig. 6 the normal contribution amounts to about 5% of the magnetic contribution at 1.2 K). The corrections are negligible for the Au:Er and Au:Tm alloys (Figs. 7 and 8).

III. THEORY

We will calculate the contribution to the magnetoresistance arising from rare-earth impurities in noble metals. We shall assume that the conduction electrons of a noble metal are in plane waves, which is a common assumption for calculating the magnetotransport properties of dilute magnetic alloys.^{7,8}

A. Scattering potential

The starting point of our calculation is a scattering potential for RE impurities in noble metals including an isotropic attractive potential, an isotropic exchange interaction, and a quadrupolar

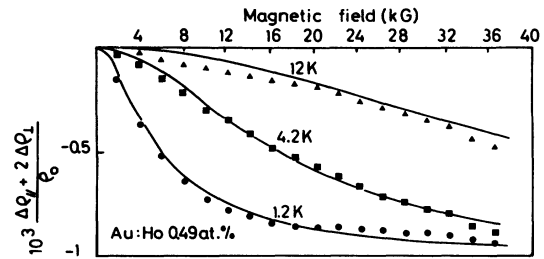


FIG. 9. Isotropic part of the magnetoresistance $[(\rho_{\parallel} - \rho_0) + 2(\rho_{\perp} - \rho_0)]/3\rho_0$ of a 0.49-at. % Au:Ho alloy versus magnetic field at several temperatures: experimental points (after a correction to eliminate the normal magnetoresistance) and calculated curves (for $x = -0.35$, $C_4 = -20$ K, $\Gamma^{(20)} = 0.042$ eV).

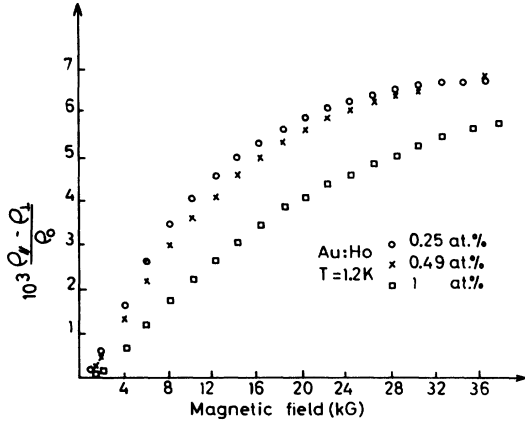


FIG. 10. Resistivity anisotropy $(\rho_{\parallel} - \rho_{\perp})/\rho_0$ of gold with 0.25, 0.49; and 1 at. % of Ho impurities versus magnetic field at 1.2 K.

Coulomb term:

$$V = V_0 + V_{\text{exch}} + V_{\text{qd}}. \quad (4)$$

The isotropic potential V_0 can be developed in terms associated with the successive spherical harmonics:

$$V_0 = 4\pi \sum_{\mathbf{l}} \frac{V^{(l)}(|k|, |k'|)}{N} \times \sum_{m\mathbf{k}\mathbf{k}'} Y_{lm}^*(\Omega_{\mathbf{k}}) Y_{lm}(\Omega_{\mathbf{k}'}) a_{\mathbf{k}\sigma}^{\dagger} a_{\mathbf{k}'\sigma}, \quad (5)$$

where $a_{\mathbf{k}}^{\dagger}$ ($a_{\mathbf{k}}$) are creation (annihilation) operators of plane waves. In a monovalent noble metal about two electrons are attracted by V_0 around a trivalent RE ion, mostly in 6s and 5d states^{9,10} (the attraction of screening electrons into 5d states is usually described as the formation of a 5d nonmagnetic virtual bound state). The partial-wave phase shifts η_l for electrons at the Fermi level are more physical parameters than the coefficients $V^{(l)}(k_F, k_F)$ because they are simply related to the screening charges Z_l by the Friedel sum rule.¹¹ Therefore we shall directly express the part of the T matrix involving only V_0 in terms of the phase shifts:

$$T_{\mathbf{k}\sigma, \mathbf{k}'\sigma'}^{(0)} = -4 \frac{\delta_{\sigma\sigma'}}{N(E_F)} \sum_{l,m} e^{i\eta_l} (\sin \eta_l) Y_{lm}^*(\Omega_{\mathbf{k}}) Y_{lm}(\Omega_{\mathbf{k}'}), \quad (6)$$

where $N(E_F)$ is the density of states (per unit of energy, unit of volume, and spin direction) in the conduction band, and where

$$\frac{2(2l+1)}{\pi} \eta_l = Z_l, \quad (7)$$

$$\sum Z_l \cong 2. \quad (8)$$

In our calculation we shall assume for simplicity that only η_0 and η_2 (or Z_0 and Z_2) are different from zero. We emphasize that $T^{(0)}$ is the dominant part of the T matrix, as is demonstrated, for example, by the nearly constant value of the residual resistivity for all the heavy RE impurities in gold (or silver), independently of the 4f spin.

V_{exch} and V_{qd} are the spin-dependent isotropic exchange term and the quadrupolar term of the Coulomb interaction between the conduction and the 4f electrons.^{4,12} V_{exch} and V_{qd} can also be expanded in terms associated to the successive spherical harmonics:

$$V_{\text{exch}} = -4\pi \sum_{\mathbf{l}} \frac{J^{(l)}}{2N} \sum_{m\mathbf{k}\mathbf{k}'} Y_{lm}^*(\Omega_{\mathbf{k}}) Y_{lm}(\Omega_{\mathbf{k}'}) \times [(a_{\mathbf{k}'}^{\dagger} a_{\mathbf{k}} - a_{\mathbf{k}'} a_{\mathbf{k}}^{\dagger}) J_z + a_{\mathbf{k}'}^{\dagger} a_{\mathbf{k}} J^- + a_{\mathbf{k}'} a_{\mathbf{k}}^{\dagger} J^+], \quad (9)$$

$$V_{\text{qd}} = 4\pi \left(J_u^2 - \frac{J(J+1)}{3} \right) \sum_{l \geq 1} \frac{D^{(l)}}{2N} \times \sum_{m\mathbf{k}\mathbf{k}'} \left(m^2 - \frac{l(l+1)}{3} \right) Y_{lm}^*(\Omega_{\mathbf{k}}) Y_{lm}(\Omega_{\mathbf{k}'}) a_{\mathbf{k}'\sigma}^{\dagger} a_{\mathbf{k}\sigma}, \quad (10)$$

where \tilde{J} is the total angular momentum of the 4f electrons and J_u its component along the axis of quantization of the spherical harmonics. As a matter of fact, V_{qd} is the axial term $O_0^2(\tilde{J})O_0^2(\tilde{l})$ of a coupling $O^2(\tilde{J})O^2(\tilde{l})$ between the irreducible tensors of rank 2, $O^2(\tilde{J})$ and $O^2(\tilde{l})$ (\tilde{l} is the orbital angular momentum of a conduction electron). The nonaxial terms are not useful for our calculation. In addition to the spin-dependent isotropic term, Eq. (9), and to the quadrupolar term, Eq. (10), the full Coulomb interaction^{4,12} includes several other terms, such as orbital exchange terms (which are important for the skew scattering problem^{3,6}), spin and orbital exchange cross terms, and direct Coulomb terms associated with multipoles of higher rank than the quadrupole. It can be shown¹³ that these additional terms do not significantly contribute to the magnetoresistance of a noble metal containing RE impurities.

If different rare earths are placed in the same host, and if it is assumed that the radial functions of the 4f and conduction electrons are the same for all of them, the coefficients $J^{(l)}$ and $D^{(l)}$ entering Eqs. (9) and (10) are given by

$$J^{(l)} = (g_J - 1) \Gamma^{(l)} \quad (11)$$

and

$$D^{(l)} = \frac{(2L+3)(2L+2)(\frac{7}{4} - S)}{(2J+3)(2J+1)(2L-1)} d^{(l)} \quad (12)$$

in the first half of the RE series and

$$D^{(l)} = \frac{L(S - \frac{7}{4})}{J(J - \frac{1}{2})} d^{(l)} \quad (13)$$

in the second half. In Eqs. (11)–(13), $\Gamma^{(l)}$ and $d^{(l)}$ are constant throughout the RE series, $g_J - 1$ is the de Gennes factor,¹⁴ and the factors preceding $d^{(l)}$ are similar scaling factors for the quadrupole interaction.¹²

The exchange interaction between conduction and localized electrons is generally assumed to be limited to its $l=0$ term. In the same way, in a previous calculation of the quadrupole scattering,¹ the quadrupole interaction V_{qd} has been restricted to its lowest term with respect to l , i.e., the $l=1$ term. However, the restriction of V_{exch} and V_{qd} to their lowest terms is not very appropriate for RE impurities in noble metals. Huang Liu, Ling, and Orbach¹⁰ have shown that the local admixture of $5d$ states into the conduction states makes the $l=2$ term of the exchange interaction dominant. In the same way Fert and Levy¹³ have shown that the largely dominant contribution to the quadrupole interaction, Eq. (10), comes from the $l=2$ term because the $5d$ admixed states lie close to the $4f$ shell and strongly feel the orbital anisotropy of the $4f$ shell. Therefore we shall restrict Eqs. (9) and (10) to their $l=2$ terms:

$$V_{exch} = -4\pi \frac{J^{(2)}}{2N} \sum_{m\vec{k}\vec{k}'} Y_{2m}^*(\Omega_{\vec{k}}) Y_{2m}(\Omega_{\vec{k}'}) \times [(a_{\vec{k}'+}^\dagger a_{\vec{k}+} - a_{\vec{k}'-}^\dagger a_{\vec{k}-}) J_z + a_{\vec{k}'+}^\dagger a_{\vec{k}-} J^- + a_{\vec{k}'-}^\dagger a_{\vec{k}+} J^+], \quad (14)$$

$$V_{qd} = 4\pi \frac{D^{(2)}}{2N} \left(J_u^2 - \frac{J(J+1)}{3} \right) \times \sum_{m\vec{k}\vec{k}'\sigma} (m^2 - 2) Y_{2m}^*(\Omega_{\vec{k}}) Y_{2m}(\Omega_{\vec{k}'}) a_{\vec{k}'\sigma}^\dagger a_{\vec{k}\sigma}. \quad (15)$$

B. Anisotropic magnetoresistance induced by quadrupole scattering

Our calculation of the resistivity will be based on the expression

$$\rho_{\vec{u}} = \frac{1}{2} \left(\frac{\hbar}{8\pi^3 n e} \right)^2 \int \left(-\frac{\partial f^0}{\partial \epsilon_{\vec{k}}} \right) (\vec{k} \cdot \vec{u}) \times [(\vec{k} - \vec{k}') \cdot \vec{u}] w_{\vec{k}\vec{k}'} d\vec{k} d\vec{k}', \quad (16)$$

where \vec{u} is a unit vector along the direction of the current, n is the number of electrons per unit volume and per spin direction, $f_{\vec{k}}^0$ is the Fermi-Dirac distribution, and $w_{\vec{k}\vec{k}'}$ is the probability of transition from \vec{k} to \vec{k}' . This expression is only valid for elastic scattering, and is obtained by using a

variational method¹⁵ with a trial distribution function

$$f_{\vec{k}} = f_{\vec{k}}^0 - \phi_{\vec{k}} \frac{\partial f^0}{\partial \epsilon_{\vec{k}}},$$

where

$$\phi_{\vec{k}} = \alpha \vec{k} \cdot \vec{u} \sim Y_{10}(\Omega_{\vec{k}}).$$

When the scattering is anisotropic, the trial function $\phi_{\vec{k}}$ should, in principle, include additional spherical harmonics of higher rank. In Appendix C we have done this and shown that such corrections to $\phi_{\vec{k}}$ lead to corrections in the resistivity that are of second order with respect to the anisotropic part of the scattering potential. However, when we allow for anisotropy in the scattering probability $w_{\vec{k}\vec{k}'}$ and keep only the isotropic term in $\phi_{\vec{k}}$, we obtain the first-order contribution to the anisotropy of the resistivity. The anisotropic part of the scattering potential is very weak as $(\rho_{\parallel} - \rho_{\perp})/\rho_0 \lesssim 2 \times 10^{-2}$. Therefore we calculate the anisotropic magnetoresistance correct to first order in the anisotropy of the scattering potential by using Eq. (16) and taking into account the anisotropy in the scattering transition probability. We write $w_{\vec{k}\vec{k}'}$ as

$$w_{\vec{k}\vec{k}'} = (2\pi/\hbar) |T_{\vec{k}\vec{k}'}^{(0)} + dT_{\vec{k}\vec{k}'}^Q|^2 \delta(\epsilon_{\vec{k}} - \epsilon_{\vec{k}'}). \quad (17)$$

$T_{\vec{k}\vec{k}'}^{(0)}$, given in Eq. (6), is the isotropic and spin-independent part of the T matrix and $dT_{\vec{k}\vec{k}'}^Q$ is the small additional contribution to the T matrix from the quadrupole interaction, Eq. (15). In contrast to $T_{\vec{k}\vec{k}'}^{(0)}$, the small contribution $dT_{\vec{k}\vec{k}'}^Q$ can be calculated in the Born approximation or, more precisely, in the distorted-wave Born approximation,¹⁶

$$dT_{\vec{k}\vec{k}'}^Q = \langle \chi_{\vec{k}'}^{(-)} | V_{qd} | \chi_{\vec{k}}^{(+)} \rangle, \quad (18)$$

in terms of the matrix elements of the quadrupole interaction between outgoing and incoming distorted waves (i.e., already distorted by the large attractive potential V_0). We obtain (see Appendix A)

$$dT_{\vec{k}\vec{k}'}^Q = 2\pi e^{2i\eta_2} \frac{D^{(2)}}{N} \left(J_u^2 - \frac{J(J+1)}{3} \right) \times \sum_m (m^2 - 2) Y_{2m}^*(\Omega_{\vec{k}}) Y_{2m}(\Omega_{\vec{k}'}). \quad (19)$$

By introducing Eqs. (6) and (19) in Eq. (17) and Eq. (17) in Eq. (16) and by integrating Eq. (16), we find that, for a concentration c of RE impurities, the contribution to the resistivity $\rho_{\vec{u}}$ which is of first order in V_{qd} is written as

$$\Delta\rho_{\vec{u}}^Q = \frac{4mcD^{(2)}}{ne^2\hbar} \sin\eta_2 (\cos\eta_2) \left(\langle J_u^2 \rangle - \frac{J(J+1)}{3} \right), \quad (20)$$

where $\langle J_u^2 \rangle$ is the thermal average of the component of \vec{J} in the direction \vec{u} of the current in a single-crystal grain and $\langle\langle J_u^2 \rangle\rangle$ is the average of $\langle J_u^2 \rangle$ on all the grain orientations. This resistivity term is anisotropic because $\langle\langle J_u^2 \rangle\rangle$ depends on the orientation of the magnetic field with respect to the current direction \vec{u} . It obviously contributes to the resistivity anisotropy $\Delta\rho_A(H)$, Eq. (2), but not to the isotropic part of the magnetoresistance $\Delta\rho_I(H)$, Eq. (3). In order to obtain the resistivity anisotropy we have to calculate $\Delta\rho_{\vec{u}}^Q$ for magnetic fields parallel and perpendicular to the current or, what must lead to the same result in a polycrystal, for two current directions \vec{u} parallel and perpendicular to a fixed field direction z . For \vec{u} parallel to z , Eq. (20) becomes

$$\Delta\rho_{\parallel}^Q = \frac{4mcD^{(2)}}{ne^2\hbar} \sin\eta_2 (\cos\eta_2) \left(\langle\langle J_z^2 \rangle\rangle - \frac{J(J+1)}{3} \right), \quad (21)$$

and for \vec{u} perpendicular to z , in a polycrystal,

$$2\langle\langle J_u^2 \rangle\rangle + \langle\langle J_z^2 \rangle\rangle = J(J+1),$$

$$\Delta\rho_{\perp}^Q = -\frac{2mcD^{(2)}}{ne^2\hbar} \sin\eta_2 (\cos\eta_2) \left(\langle\langle J_z^2 \rangle\rangle - \frac{J(J+1)}{3} \right). \quad (22)$$

It follows that the contribution to the fractional resistivity anisotropy is expressed as

$$\frac{\rho_{\parallel} - \rho_{\perp}}{\rho_0} = 6\pi n(E_F)D^{(2)} \frac{\sin\eta_2 \cos\eta_2}{\sin^2\eta_0 + 5\sin^2\eta_2} \times \left(\langle\langle J_z^2 \rangle\rangle - \frac{J(J+1)}{3} \right), \quad (23)$$

where $n(E_F)$ is the density of states at the Fermi level (per unit energy, per atom and spin direction), and ρ_0 is the zero-field resistivity that we suppose mostly induced by $T^{(0)}$ and thus given by

$$\rho_0 = \frac{mc}{\pi ne^2\hbar n(E_F)} (\sin^2\eta_0 + 5\sin^2\eta_2). \quad (24)$$

We emphasize that, in Eq. (23), $\langle\langle J_z^2 \rangle\rangle$ is a thermal and powder average of the square component of \vec{J} in the field direction.

C. Crystal-field effects on the anisotropic magnetoresistance

The quadrupole-moment polarization $\langle\langle J_z^2 \rangle\rangle - \frac{1}{3}J(J+1)$ entering the expression of the resistivity anisotropy, Eq. (23), depends on the field and on the temperature in very different ways according to the scheme of crystal-field splitting for the RE ion.

If the ground state is a triplet or a quartet, different values of J_z^2 are associated with the states of the triplet or of the quartet, and the Zeeman

splitting of the ground state directly results in a contribution to the resistivity anisotropy, Eq. (23). This contribution is obviously proportional to $(\mu_B H/k_B T)^2$ in the low-field limit. Then one expects a saturation of the resistivity anisotropy *within the ground state* for $\mu_B H \gtrsim k_B T$ and, after this partial saturation, a generally slow increase due to the admixture of excited states, up to a complete saturation ($\langle\langle J_z^2 \rangle\rangle = J^2$) at very high field.

If the ground state is a Kramers doublet, J_z^2 is equal to $\frac{1}{3}J(J+1)$ for both states of the doublet (as for a spin $\frac{1}{2}$), and the resistivity anisotropy can result only from the admixture of excited states into the states of the doublet by the magnetic field. It can be easily shown that, as long as $\mu_B H$ is very small compared to the energy difference Δ between the ground and excited states, the quadrupole moment induced by mixing is proportional to $\mu_B H/\Delta$ and has a different sign for the two states of the doublet:

$$\langle\langle J_z^2 \rangle\rangle - \frac{1}{3}J(J+1) \sim \pm \mu_B H/\Delta. \quad (25)$$

It immediately results from Eq. (23) that

$$\frac{\rho_{\parallel} - \rho_{\perp}}{\rho_0} \sim (n_+ - n_-) \frac{\mu_B H}{\Delta} \sim \langle\langle J_z \rangle\rangle \frac{\mu_B H}{\Delta}, \quad (26)$$

where n_+ and n_- denote the populations of the states of the doublet. At low temperature

$$\frac{\rho_{\parallel} - \rho_0}{\rho_0} \sim \frac{(\mu_B H)^2}{k_B T \Delta} \quad \text{for } \mu_B H \ll k_B T \ll \Delta,$$

$$\sim \frac{\mu_B H}{\Delta} \quad \text{for } k_B T \lesssim \mu_B H \ll \Delta.$$

With respect to the case of a triplet or a quartet ground state, the initial variation in $H^2 T^{-2}$ is replaced by a variation in $H^2 T^{-1}$ and the partial saturation for $\mu_B H > k_B T$ by a variation which is temperature independent and linear in H .

If the ground state is a singlet, the quadrupole moment is also induced by admixture of excited states into the ground state. It can be easily shown that, at low field, the quadrupole moment appears in a second-order perturbation calculation:

$$\langle\langle J_z^2 \rangle\rangle - \frac{1}{3}J(J+1) \sim (\mu_B H/\Delta)^2. \quad (27)$$

It follows that a resistivity anisotropy proportional to H^2 and independent of T is expected, at least as long as $k_B T$ and $\mu_B H$ are much smaller than Δ .

We shall see in Sec. IV that these typical behaviors for triplet or quartet, Kramers doublet, and singlet ground states, respectively, are observed in the experimental results. Of course, there are some more complicated cases with, for example, several low-lying levels in a small energy range.

D. Isotropic magnetoresistance induced by exchange scattering

The negative isotropic magnetoresistance of dilute magnetic alloys has been calculated by several authors.^{7,8} The conventional starting point is a scattering potential limited to $l=0$ terms:

$$V = V_0 + V_{\text{exch}}, \quad (28)$$

$$V_0 = \sum_{\vec{k}\vec{k}'} \frac{V^{(0)}}{N} a_{\vec{k}}^\dagger a_{\vec{k}'}, \quad (29)$$

$$V_{\text{exch}} = - \sum_{\vec{k}\vec{k}'} \frac{J^{(0)}}{2N} [(a_{\vec{k}'}^\dagger a_{\vec{k}+}^\dagger - a_{\vec{k}'}^\dagger a_{\vec{k}-}^\dagger) J_z + a_{\vec{k}'}^\dagger a_{\vec{k}-}^\dagger J^- + a_{\vec{k}'}^\dagger a_{\vec{k}+}^\dagger J^+]. \quad (30)$$

If $J^{(0)}$ is much smaller than $V^{(0)}$ and in the Born approximation the result of Beal-Monod and Weiner⁸ is written in our notation, we have

$$\frac{\Delta\rho_I(H)}{\rho_0} = - \left(\frac{J^{(0)}}{V^{(0)}} \right)^2 \left[\langle (J_z)^2 \rangle + \frac{1}{4} | \langle J_z \rangle | \times \left(\coth \frac{1}{2}\alpha - \frac{\frac{1}{2}\alpha}{\sinh^2 \frac{1}{2}\alpha} \right) \right], \quad (31)$$

where $\alpha = g_J \mu_B H / k_B T$. The first term in the square bracket arises from scattering without spin-flip by the part $s_z J_z$ of V_{exch} . The second term arises from the spin-flip processes and generally is much smaller. For example, in the high-field limit, the first term equals J^2 and the second $\frac{1}{4}J$. The first term is still more predominant at low field. As Eq. (31) is to be applied to RE impurities with large values of J and specially to Ho^{+3} ($J=8$, $J^2=64$, $\frac{1}{4}J=2$), we can neglect the second term of Eq. (31) and write the simplified expression

$$\Delta\rho_I(H)/\rho_0 = -(J^{(0)}/V^{(0)})^2 \langle (J_z)^2 \rangle. \quad (32)$$

The calculation of Beal-Monod and Weiner assumes free localized moments (no crystal field). In the presence of crystal field, Eq. (32) for the contribution of the non-spin-flip scattering still holds, except that, in a polycrystal, $\langle (J_z)^2 \rangle$ is replaced by $\langle \langle (J_z)^2 \rangle \rangle$ [average of $\langle (J_z)^2 \rangle$ on all the orientations of the crystal axes with respect to the direction O_z of the field]:

$$\Delta\rho_I(H)/\rho_0 = -(J^{(0)}/V^{(0)})^2 \langle \langle (J_z)^2 \rangle \rangle. \quad (33)$$

However, for RE impurities in noble metals, the scattering potential cannot be limited to the $l=0$ terms and, at least for its isotropic part V_0 , cannot be treated in Born approximation. For the isotropic part V_0 we have to introduce the matrix elements $T_{\vec{k}\vec{k}'}^{(0)}$, Eq. (6), in place of $V^{(0)}/N$ in Eq. (29). For the exchange interaction, Eq. (30) is to be replaced by Eq. (14) and, as is shown in Appendix A, its contribution to the non-spin-flip elements of T matrix is

$$dT_{\vec{k}\vec{k}'}^{E_2} = 2\pi e^{2i\eta_2} (g_J - 1) \frac{\Gamma^{(2)}}{N} \langle J_z \rangle \times \sum_m Y_{2m}^*(\Omega_{\vec{k}}) Y_{2m}(\Omega_{\vec{k}'}). \quad (34)$$

After a calculation exactly similar to that of Beal-Monod and Weiner,⁸ we find in place of Eq. (33)

$$\frac{\Delta\rho_I(H)}{\rho_0} = - \left(5\pi (g_J - 1) \Gamma^{(2)} n(E_F) \times \frac{\sin\eta_2 \cos\eta_2}{\sin 2\eta_0 + 5 \sin^2 \eta_2} \right)^2 \langle \langle (J_z)^2 \rangle \rangle. \quad (35)$$

IV. DISCUSSION OF THE EXPERIMENTAL RESULTS

A. Sign of the resistivity anisotropy

From Eqs. (13) and (23) the resistivity anisotropy is expected to be proportional to $L(S - \frac{7}{4})$ for heavy RE impurities. We just observe in the experimental results (Figs. 1–8) that the resistivity anisotropy vanishes for Gd impurities ($L=0$), and is positive for Tb, Dy, and Ho ($S > \frac{7}{4}$) and negative for Er and Tm ($S < \frac{7}{4}$). This agreement demonstrates that *the resistivity anisotropy is mainly due to quadrupole scattering*. It can be noticed that the contributions from multipoles of higher order should not present more than one change of sign in the series of the heavy RE. These contributions are apparently too small to modify the typical variation of sign of the contribution from quadrupole scattering. We also point out that the resistivity anisotropy observed for Au:Yb is negative, in agreement with what is expected. However, the model of this paper should not be appropriate for Yb impurities in Au for which a strong interaction from covalent mixing exists. A different model based on the covalent mixing mechanism also predicts the negative sign. It will be presented elsewhere together with the experimental results for Au:Yb.

B. Crystal-field effects

Figures 1–8 show the different behaviors observed for different schemes of crystal-field levels.

The temperature and field dependence of the resistivity anisotropy $(\rho_{\parallel} - \rho_{\perp})/\rho_0$ of Au:Ho alloys (Fig. 6) is similar to what is expected for a triplet or a quartet ground state: variation in $H^2 T^{-2}$ at low field and saturation (within the ground state) at high field and low temperature ($H > 20$ kG at 1.2 K in Fig. 6). This behavior is accounted for by the crystal-field level scheme found by Murani¹⁷: a $\Gamma_4^{(2)}$ triplet lies a few tenths of K above the non-magnetic ground state and therefore is populated in

our experimental temperature range. In Sec. V we will determine the crystal-field parameters from the field and temperature dependence of the resistivity anisotropy of the Au:Ho alloys.

The resistivity anisotropy of Au:Er (Fig. 7) is approximately proportional to H^2/T at low field; then, at least at low temperature, between 1.2 and 4.2 K, it is approximately proportional to H and is weakly temperature dependent. This is the behavior expected when the ground state is a Kramers doublet, in agreement with the existence of a Γ_7 ground state for the Au:Er system.¹⁸

The resistivity anisotropy of Au:Tm (Fig. 8) is temperature independent below 4.2 K and approximately proportional to H^2 below about 20 kG. This is the characteristic behavior for a singlet ground state at low temperature and low field, in agreement with a ground state for Tm in Au (Ref. 19) (our results suggest that Δ is small).

The behavior of the resistivity anisotropy of Au:Tb (Fig. 2) is not really similar to one of three typical behaviors described in Sec. III C. This is certainly related to a complicated level scheme with several low-lying levels in an energy range of few K.²⁰

The resistivity anisotropy $(\rho_{\parallel} - \rho_{\perp})/\rho_0$ of Au:Dy alloys strongly depends on the concentration of Dy. We will discuss these concentration effects in Sec. IV C.

C. Concentration effects

We have generally observed that the resistivity anisotropy of our alloys is approximately independent of the RE concentration. However, concentration effects are observed in some systems.

Figure 10 shows the resistivity anisotropy at 1.2 K for gold alloys containing 0.25, 0.49, and 1 at. % of Ho impurities. It can be seen that the resistivity anisotropy of the lower concentrations (0.25 and 0.49 at. %) is nearly independent of the concentration (which is expected for noninteracting impurities). Concentration effects become apparent for 1 at. % of Ho: the resistivity anisotropy is smaller and increases more progressively.

Similar concentration effects are observed for the Au:Dy alloys: for a 1.4-at. % concentration (Fig. 3) the resistivity anisotropy is approximately linear in H and temperature independent for large enough values of H/T , which is consistent with a Kramers-doublet ground state; in contrast, for a 0.3-at. % concentration we have observed a larger anisotropy, with a tendency to saturation above 30 kG at 1.2 K, which rather suggests a quartet ground state.

Our results on Au:Dy alloys are apparently in

agreement with those of Chelkowski and Orbach.²¹ They interpret concentration effects on the magnetic susceptibility of Au:Dy by a small change of the crystal-field parameters and a resulting reversal of the ground state from a $\Gamma_8^{(1)}$ quartet at low concentration into a Γ_7 doublet above about 0.5 at. %. However, such an interpretation could not account for the definite concentration effects that we have observed in Au:Ho alloys: we have computed that, in this case, a small change of the crystal-field parameters weakly affects $\langle\langle J_z^2 \rangle\rangle$ and the resistivity anisotropy. We are rather inclined to ascribe the concentration effects to a noncubic "crystal field" due to the lattice distortion by the neighbor impurities. Such a noncubic component would split triplet or quartet levels. This could explain the importance of concentration effects on the resistivity anisotropy when a triplet (Ho) or a quartet (Dy) is involved.

V. ANALYSIS OF THE MAGNETORESISTANCE OF Au:Ho ALLOYS

We consider the experimental results obtained for Au:Ho alloys in the concentration range (below 0.5 at. %) where the magnetoresistance induced by the Ho impurities is practically concentration independent. Figure 6 shows the anisotropic part of the magnetoresistance, i.e., the resistivity anisotropy $(\rho_{\parallel} - \rho_{\perp})/\rho_0$, and Fig. 9 shows the isotropic part, $[(\rho_{\parallel} - \rho_0) + 2(\rho_{\perp} - \rho_0)]/3\rho_0$.

Equations (23) and (35) give the anisotropic and isotropic contributions to the magnetoresistance from quadrupole scattering and from exchange scattering, respectively. In order to fit Eqs. (23) and (35) with the experimental results of Figs. 6 and 9 we have calculated $\langle\langle J_z^2 \rangle\rangle$ and $\langle\langle (J_z)^2 \rangle\rangle$ for several values of the crystal-field parameters x and C_4 . This calculation is described in Appendix B. The best fit with the experimental field and temperature dependences is obtained for

$$x = -0.35, \quad C_4 = -20 \text{ K}.$$

The agreement is good for both the anisotropic part, Fig. 6, and the isotropic part, Fig. 9, of the magnetoresistance. The crystal-field parameters are close to those obtained for Ho in Au by Murani¹⁷ from susceptibility measurements. The magnitude of the experimental effects is accounted for by putting in Eqs. (13), (23), and (35) $n(E_F) = 0.15$ states per eV, atom and spin, $\eta_0 = \frac{1}{2}\pi$, $\eta_2 = \frac{1}{10}\pi$ (i.e., $Z_0 = Z_2 = 1$),²² and

$$d^{(2)} = 0.020 \text{ eV (anisotropic part)},$$

$$\Gamma^{(2)} = 0.042 \text{ eV (isotropic part)}.$$

The values found for $d^{(2)}$ and $\Gamma^{(2)}$ do not strongly depend on the choice of x , C_4 , Z_0 , and Z_2 . For

example, if C_4 shifts to -30 K, the variation of $d^{(2)}$ and $\Gamma^{(2)}$ is smaller than 10%, and if x varies between -0.3 and -0.4 , the variation of $d^{(2)}$ and $\Gamma^{(2)}$ is smaller than 5%. In the same way, if Z_2 varies between 0.5 and 2 (Z_0 varying between 1.5 and 0), $d^{(2)}$ varies between 0.018 and 0.026 eV and $\Gamma^{(2)}$ varies between 0.041 and 0.058 eV; if a screening charge $Z_1 = 0.2$ is introduced (with $Z_0 = Z_2 = 0.9$), the variation of $d^{(2)}$ and $\Gamma^{(2)}$ is smaller than 10%. We remark that the values of $\Gamma^{(2)}$ found for Gd impurities in Au are not very different: 0.041 eV from the magnetoresistance and about 0.11 eV from EPR data (see Sec. VI). Finally we point out that, because of a numerical error, we gave in a previous publication³ an erroneous value of $d^{(2)}$: 0.049 instead of 0.020 eV.

VI. ANALYSIS OF THE ISOTROPIC MAGNETORESISTANCE OF Au:Gd ALLOYS

The Au:Gd alloys (Fig. 1) exhibit the conventional negative and isotropic magnetoresistance induced by exchange scattering. For Gd impurities ($J = \frac{7}{2}$, $g_J = 2$) we write

$$\langle J_x \rangle = JB_{7/2}(2\mu_B H/k_B T),$$

where $B_{7/2}(x)$ is the Brillouin function for $J = \frac{7}{2}$, and Eq. (35) becomes

$$\frac{\Delta\rho_I(H)}{\rho_0} = - \left(\frac{5\pi J \Gamma^{(2)} n(E_F) \sin\eta_2 \cos\eta_2}{\sin^2\eta_0 + 5\sin^2\eta_2} \right)^2 \times \left[B_{7/2} \left(\frac{2\mu_B H}{k_B T} \right) \right]^2. \quad (36)$$

The best fit of Eq. (36) with the experimental results of Fig. 1 has been obtained by using the values of Z_0 , Z_1 , and $n(E_F)$ already used in Sec. V and $\Gamma^{(2)} = 0.041$ eV. This value of $\Gamma^{(2)}$ does not strongly depend on the choice of Z_0 and Z_2 . It can be noted that this value of the exchange coefficient $\Gamma^{(2)}$ is not very different from the value found for the Ho impurities in Sec. V.

We can also compare the value found for $\Gamma^{(2)}$ with the values derived from reflection electron spin resonance (RESR) experiments on Au:Gd alloys. If we assume with Huang Liu *et al.*¹⁰ that the predominant term of the exchange interaction is the $l=2$ term, the exchange interaction can be limited to its $l=2$ terms and is given²³ by Eq. (9). The exchange broadening and the g shift of the unbottlenecked resonance is then given, after Davidov *et al.*,²⁴ by

$$\Delta H = \frac{5}{4} (\pi k_B T / g \mu_B) [\Gamma^{(2)} n(E_F)]^2, \quad (37)$$

$$\Delta g = \frac{5}{2} \Gamma^{(2)} n(E_F). \quad (38)$$

Chock *et al.*²⁵ give for the RESR of Gd impurities in gold

$$\Delta H / \Delta T = 8 \text{ K/G}, \quad g = 2.05 \quad (\Delta g \approx 0.05),$$

which, in their interpretation of an unbottleneck resonance, yields, after (37) and (38), $\Gamma^{(2)} = 0.11$ eV and $\Gamma^{(2)} = 0.13$ eV [note that (37) and (38) still hold if the RESR signal is identified with a high-wave-vector resonance, as in the similar Ag:Gd system²⁶]. The values of $\Gamma^{(2)}$ found from RESR are about three times larger than the value derived from the magnetoresistance of Au:Gd. However, the introduction of an exchange constant $\Gamma^{(0)}$ for the s partial waves in the analysis would bring the values of $\Gamma^{(2)}$ derived from the RESR much nearer to the value derived from the magnetoresistance (because the contribution from $\Gamma^{(0)}$ would be much more significant to $\Delta H / \Delta T$ and to Δg than to the magnetoresistance $\Delta\rho_I$, as can be easily shown).

VII. DISCUSSION

We will mainly discuss the data obtained on the quadrupole interaction. We have found in Sec. V $d^{(2)} = 0.020$ eV and $\Gamma^{(2)} = 0.042$ eV for Ho impurities in gold. The direct comparison of the magnitude of $d^{(2)}$ and $\Gamma^{(2)}$ is not very significant, because the quadrupole and exchange interactions, Eqs. (10) and (9), respectively, also involve large numerical coefficients. It is more relevant to compare the amplitude of variation of these interaction terms, i.e., the characteristic energies

$$E_{\text{qd}} = 5L(S - \frac{7}{4})d^{(2)}, \quad E_{\text{is. exch.}} = 5S\Gamma^{(2)}.$$

For Ho impurities we obtain

$$E_{\text{qd}} = 0.15 \text{ eV}, \quad E_{\text{is. exch.}} = 0.42 \text{ eV}.$$

We have also calculated E_{qd} and $E_{\text{is. exch.}}$ for the other heavy-RE impurities by assuming that the scaling laws (11) and (13), with $\Gamma^{(2)}$ and $d^{(2)}$ constant in the RE series, are obeyed (which turns out to be approximately observed in our experimental result). The values obtained for E_{qd} and $E_{\text{is. exch.}}$ are plotted in Fig. 11. The interesting result is that the quadrupole interaction has the same order of magnitude as the spin-dependent isotropic exchange interaction (the quadrupole interaction is even larger for Tm impurities). We have seen in Sec. V that reasonable changes of the other parameters entering the analysis do not strongly modify the values obtained for $d^{(2)}$. It follows that our results reliably demonstrate the importance of the quadrupole interaction for RE impurities in gold. The orbital exchange interaction (of $\mathbf{l} \cdot \mathbf{L}$ type),

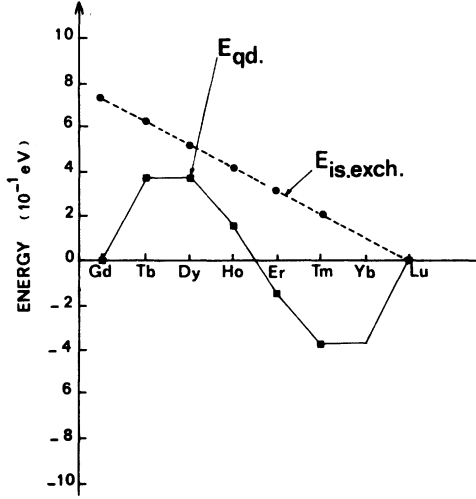


FIG. 11. Characteristic energies of the quadrupole interaction (E_{qd}) and of the isotropic exchange interaction ($E_{is.exch.}$) for heavy-RE impurities in gold. We have presented in a previous paper (Ref. 3) an erroneous plot in which the values of E_{qd} have to be scaled down by a factor 2.4.

which has been determined in the same alloys from the skew scattering effect, is found to be smaller by about an order of magnitude.³ Thus the quadrupole interaction turns out to be the leading anisotropic term and the only one which reaches the order of magnitude of the isotropic exchange.

The quadrupole interaction has also been determined for RE impurities in gadolinium by Azomoza *et al.*² and has been found to be several times smaller than the isotropic exchange. What is the origin of the specially large quadrupole interaction found for RE impurities in gold? Fert and Levy¹³ have accounted for this large quadrupole interaction by the admixture of $5d$ states (localized on the RE) into the conduction band: because the $5d$ electrons lie close to the $4f$ electrons, the conduction electrons can strongly feel the orbital anisotropy of the $4f$ shell.

VIII. CONCLUSION

Rare-earth impurities in gold (with the exception of Gd) induce an anisotropic magnetoresistance which is clearly due to quadrupole scattering. The analysis of the experimental results provides interesting information on the interaction of the conduction electrons of gold with the $4f$ electrons. We find that this quadrupole interaction has the same order of magnitude as the exchange interaction. Other studies of scattering by $4f$ quadrupoles would be of interest to obtain the magnitude of the quadrupole interaction in various systems. Information

on this magnitude should be useful to understand the role of the Ruderman-Kittel-Kasuya-Yosida biquadratic interaction in the magnetic properties of the rare-earth metals and compounds.

ACKNOWLEDGMENTS

We thank J. Sierro and A. P. Murani, who provided us with many of the specimens studied in this paper. We acknowledge numerous discussions with P. M. Levy and H. Hurdequint.

APPENDIX A

In the distorted-wave Born approximation¹⁶ the contribution to the T matrix from a small scattering potential dV added to the main scattering potential V_0 is written as

$$dT_{\mathbf{k}\mathbf{k}'}^{(\pm)} = \langle \chi_{\mathbf{k}}^{(\pm)} | dV | \chi_{\mathbf{k}'}^{(\pm)} \rangle, \quad (\text{A1})$$

where $\chi_{\mathbf{k}}^{(\pm)}$ ($\chi_{\mathbf{k}}^{(-)}$) are outgoing (incoming) distorted waves. If the incident waves, before being distorted by V_0 , are plane waves, and if η_l are the phase shifts associated to the scattering by V_0 , $\chi_{\mathbf{k}}^{(\pm)}$ are written as

$$\chi_{\mathbf{k}}^{(\pm)} = 4\pi \sum_l i^l e^{\pm i\eta_l} \varphi_l(k, r) \sum_m Y_{lm}^*(\Omega_{\mathbf{k}}) Y_{lm}(\Omega_{\mathbf{k}}). \quad (\text{A2})$$

With respect to the similar expansion of a plane wave, i.e.,

$$\chi_{\mathbf{k}} = 4\pi \sum_l i^l j_l(kr) \sum_m Y_{lm}^*(\Omega_{\mathbf{k}}) Y_{lm}(\Omega_{\mathbf{k}}), \quad (\text{A3})$$

the distorted radial functions $\varphi_l(k, r)$ replace the Bessel function $j_l(kr)$ and phase factors $e^{\pm i\eta_l}$ turn up.

If dV is, for example, the $l=2$ quadrupole term of the Coulomb interaction of the conduction electrons with the $4f$ shell, the matrix elements of V_{qd} between plane waves and distorted waves are, respectively,

$$\begin{aligned} \langle \chi_{\mathbf{k}} | V_{qd} | \chi_{\mathbf{k}'} \rangle &= 2\pi \frac{D_{\text{PW}}^{(2)}}{N} \left(J_u^2 - \frac{J(J+1)}{3} \right) \\ &\times \sum_m (m^2 - 2) Y_{2m}^*(\Omega_{\mathbf{k}}) Y_{2m}(\Omega_{\mathbf{k}'}), \quad (\text{A4}) \end{aligned}$$

$$\begin{aligned} dT_{\mathbf{k}\mathbf{k}'}^{(0)} &= \langle \chi_{\mathbf{k}}^{(0)} | V_{qd} | \chi_{\mathbf{k}'}^{(0)} \rangle \\ &= 2\pi e^{2i\eta_2} \frac{D_{\text{DW}}^{(2)}}{N} \left(J_u^2 - \frac{J(J+1)}{3} \right) \\ &\times \sum_m (m^2 - 2) Y_{2m}^*(\Omega_{\mathbf{k}}) Y_{2m}(\Omega_{\mathbf{k}'}), \quad (\text{A5}) \end{aligned}$$

where $D_{\text{PW}}^{(2)}$ and $D_{\text{DW}}^{(2)}$ are related to Coulomb integrals which involve, respectively, Bessel functions and distorted radial functions. Our calculations of Sec. III B is based on Eq. (A5), and there-

fore, throughout the paper, the coefficient $D^{(2)}$ (or $d^{(2)}$) is the coefficient $D_{\text{DW}}^{(2)}$ (or $d_{\text{DW}}^{(2)}$ for distorted waves. In the same way the contribution to the T matrix to the non-spin-flip exchange scattering is written

$$dT_{kk'}^E = 2\pi e^{2i\eta_2} (g_J - 1) \frac{\Gamma^{(2)}}{N} \langle J_z \rangle \sum_m Y_{2m}^*(\Omega_{\mathbf{k}'}) Y_{2m}(\Omega_{\mathbf{k}}), \quad (\text{A6})$$

where $\Gamma^{(2)}$ is associated with exchange involving distorted radial functions.

Fert and Levy¹³ show that, for $4f$ ions in noble metals, the $l=2$ Coulomb and exchange constants calculated with distorted waves are much larger than those calculated with plane waves.

APPENDIX B

By using the notation of Lea *et al.*,²⁷ the crystal-field Hamiltonian in cubic symmetry can be written as

$$H_c = W \left(\frac{x}{F(4)} (O_4^0 + 5O_4^4) + \frac{1-|x|}{F(6)} (O_6^0 - 21O_6^4) \right). \quad (\text{B1})$$

We have the axis of quantization along the fourfold axis of the crystal. When an external magnetic field H is applied, the full Hamiltonian is

$$H = H_c + g \mu_B \vec{\mathbf{J}} \cdot \vec{\mathbf{H}}. \quad (\text{B2})$$

We call u and E_u the eigenstates and energies of H .

We expand the density matrix of the level J in a tensor-operator basis,²⁸

$$\rho = \sum_{kq} T_k^{q\dagger}(J) \rho_k^q \quad (\text{B3})$$

or

$$\rho_k^q = \text{Tr}(\rho T_k^q). \quad (\text{B4})$$

As the density matrix is diagonal in the eigenstate basis, we can write it as

$$\rho_k^q = \sum_u \rho_u \langle u | T_k^q | u \rangle, \quad (\text{B5})$$

where ρ_u is the population of the state u . This is given at each temperature by the Boltzmann factor:

$$\rho_u = \frac{\exp(-E_u/k_B T)}{\sum_u \exp(-E_u/k_B T)}. \quad (\text{B6})$$

It should be noted that the densities ρ_k^q are taken along the quantization axis z and not along the direction of the magnetic field. Therefore to determine the densities along the direction of the field we must perform a rotation w . The tensor operators T_k^q are transformed into $T_k'^q$, and the densities referred to the field direction, i.e., σ_k^q , are given by

$$\sigma_k^q = \text{Tr}(\rho T_k'^q) \quad (\text{B7})$$

$$= \text{Tr} \rho \sum_{q'=-k}^{+k} \mathcal{D}_{q'q}^k(\omega) T_k^{q'} \quad (\text{B8})$$

$$= \sum_{q'=-k}^{+k} \mathcal{D}_{q'q}^k(\omega) \rho_k^{q'}, \quad (\text{B9})$$

where $\mathcal{D}_{q'q}^k(\omega)$ are the matrix elements of the rotation operator. In the special cases considered here, where $q=0$, one finds

$$\sigma_k^0 = \sum_{q'=-k}^{+k} (-)^{q'} \left(\frac{4\pi}{2k+1} \right)^{1/2} Y_{kq'}(\omega) \rho_k^{q'}, \quad (\text{B10})$$

where Y_{kq} are usual spherical harmonics.

For polycrystalline samples in which the applied field takes all directions with respect to the crystal-field axis, one must perform an average over all these directions. In practice we considered 9×16 directions. As a test of the accuracy we considered 36×16 directions for a given magnitude of the field and we observed that none of the results changed by more than 1%.

APPENDIX C

Here we consider the resistivity due to scattering by an anisotropic potential and apply the variational method of Ziman.²⁹ In presence of anisotropic scattering, the trial function $\phi_{\mathbf{k}}$ must include spherical harmonics of rank higher than 1. For simplicity we assume that the anisotropy is due to an interaction with quadrupoles of axis x with the current along z . The trial function to be used in this case is written as

$$\phi_{\mathbf{k}} = \eta_1 \phi_1 + \eta_2 \phi_2, \quad (\text{C1})$$

where

$$\phi_1 = \cos \theta_{\mathbf{k}} \sim \vec{\mathbf{k}} \cdot \vec{\mathbf{u}} \sim Y_{10}(\Omega_{\mathbf{k}}), \quad (\text{C2})$$

$$\phi_2 = \cos \theta_{\mathbf{k}} \sin^2 \theta_{\mathbf{k}} \cos 2\phi_{\mathbf{k}} \sim (Y_{3,2} + Y_{3,-2}). \quad (\text{C3})$$

According to Ziman, the application of the variation principle in the general case, i.e., for $\phi_{\mathbf{k}} = \sum_i \eta_i \phi_i$, yields the following expression for the conductivity³⁰:

$$\sigma = \rho^{-1} = \sum_i X_i (P^{-1})_{ij} X_j. \quad (\text{C4})$$

The matrix P and the vector \vec{X} are defined by Ziman.²⁹ In our case we have

$$\begin{aligned} X_2 &\sim \int \cos \theta_{\mathbf{k}}^2 \sin^3 \theta_{\mathbf{k}} \cos 2\phi_{\mathbf{k}} d\theta_{\mathbf{k}} d\phi_{\mathbf{k}} \\ &\sim \int \cos 2\phi_{\mathbf{k}} d\phi_{\mathbf{k}} = 0. \end{aligned}$$

Then, the expression for the conductivity reduces to

$$\sigma = \rho^{-1} = (X_1)^2 (P^{-1})_{11} = \frac{X_1^2}{P_{11} - P_{12}^2/P_{22}}, \quad (C5)$$

where P_{12} is given as

$$P_{12} \sim \int (\cos \theta_{\mathbf{k}} - \cos \theta_{\mathbf{k}'}) \times w_{\mathbf{k}\mathbf{k}'} (\cos \theta_{\mathbf{k}} \sin^2 \theta_{\mathbf{k}'} \cos 2\phi_{\mathbf{k}} - \cos \theta_{\mathbf{k}'} \sin^2 \theta_{\mathbf{k}} \cos 2\phi_{\mathbf{k}'}) d\Omega_{\mathbf{k}} d\Omega_{\mathbf{k}'}. \quad (C6)$$

If $w_{\mathbf{k}\mathbf{k}'}$ is isotropic, it is easy to show that P_{12} is zero, and Eq. (C5) reduces to

$$\sigma = \rho^{-1} = X_1^2/P_{11}. \quad (C7)$$

However, if $w_{\mathbf{k}\mathbf{k}'}$ includes an anisotropic term, P_{12}

is nonzero and proportional to the anisotropic part of the scattering potential. When we limit our calculation to terms which are first order in the anisotropic part of the scattering potential, we can neglect P_{12}^2/P_{22} in Eq. (C5). By allowing for anisotropy in the transition probability $w_{\mathbf{k}\mathbf{k}'}$ in Eq. (C7), i.e., Eq. (16) of this paper, we obtain an anisotropic contribution to P which is first order with respect to the anisotropic part of the scattering potential.

In the general case (no special orientation of the quadrupole) ϕ_2 is a more complicated combination of spherical harmonics, but one arrives at the same conclusions.

*Supported in part by Grant No. 75-7-1155 from the Delegation Générale à la Recherche Scientifique.

†On leave of absence from Argentine National Research Council (CONICET).

‡Associé au Centre National de la Recherche Scientifique.

¹A. Friederich and A. Fert, Phys. Rev. Lett. **33**, 1214 (1974); A. Fert and A. Friederich, AIP Conf. Proc. **24**, 466 (1975).

²R. Asomoza, G. Creuzet, A. Fert, and R. Reich, Solid State Commun. **18**, 905 (1976); J. Bijvoet, G. Merlijn, and P. Frings, Physica (Utr.) **86-88B**, 535 (1977).

³A. Fert, Physica (Utr.) **86-88B**, 491 (1977).

⁴H. H. Teitelbaum and P. M. Levy, Phys. Rev. B **14**, 3058 (1976); M. J. Sablik, H. H. Teitelbaum, and P. M. Levy, AIP Conf. Proc. **10**, 548 (1973).

⁵B. Lüthi, H. E. Mullen, K. Andres, E. Bucher, and J. P. Maita, Phys. Rev. B **9**, 2639 (1973); J. Sierro, E. Bucher, L. D. Longinotti, H. Takayama, and P. Fulde, Solid State Commun. **17**, 79 (1975).

⁶A. Fert and A. Friederich, Phys. Rev. B **13**, 397 (1976).

⁷T. Van Peski Tinbergen and A. J. Dekker, Physica (Utr.) **84B**, 67 (1976).

⁸M. T. Beal-Monod and R. A. Weiner, Phys. Rev. **170**, 552 (1968).

⁹H. Chow, Phys. Rev. B **7**, 3404 (1973); R. Devine, J. Phys. F **4**, 1447 (1974); D. Sang and A. Myers, J. Phys. F **6**, 545 (1976); F. F. Bekker and T. P. Hoogkaner, Physica (Utr.) **84B**, 67 (1976).

¹⁰N. L. Huang Liu, J. K. Ling, and R. Orbach, Phys. Rev. B **14**, 4087 (1976).

¹¹E. Daniel and J. Friedel, in *Proceedings of the Ninth International Conference on Low Temperature Physics*, edited by J. Daunt, P. Edwards, F. Milford, and M. Yaquib (Plenum, New York, 1965), p. 933.

¹²T. Kasuya and D. H. Lyons, J. Phys. Soc. Jpn. **12**, 287 (1966); J. Kondo, Prog. Theor. Phys. **25**, 722 (1962); L. L. Hirst, Z. Phys. **244**, 230 (1971).

¹³A. Fert and P. M. Levy, Phys. Rev. B **16**, 5052 (1977)

(following paper).

¹⁴P. G. de Gennes, C. R. Acad. Sci. **247**, 836 (1966).

¹⁵J. M. Ziman, *Electrons and Phonons* (Clarendon, Oxford, 1960).

¹⁶A. Messiah, *Mécanique Quantique* (Dunod, Paris, 1964); see Sec. XIX-11.

¹⁷A. P. Murani, J. Phys. F Suppl. **2**, S153 (1970).

¹⁸D. Davidov, C. Rettori, A. Dixon, K. Baberscke, E. P. Chock, and R. Orbach, Phys. Rev. B **8**, 3563 (1973).

¹⁹G. Williams and L. L. Hirst, Phys. Rev. **185**, 407 (1969).

²⁰J. A. Barclay and B. Perczuk, Solid State Commun. **17**, 565 (1975).

²¹A. Chelkowski and R. Orbach, Phys. Rev. B **12**, 208 (1975).

²²The choice $Z_0 = Z_2 = 1$ correctly accounts for the residual resistivity of RE impurities in gold ($\rho_0 \approx 7 \mu\Omega \text{ cm/at. } \%$). These values of Z_0 and Z_2 have been also used by Chow (Ref. 9) to account for the crystal-field parameters and by Huang Liu *et al.* (Ref. 10) in the interpretation of EPR data.

²³Only isotropic exchange exists for Gd impurities ($L = 0$).

²⁴D. Davidov, K. Maki, R. Orbach, F. Rettori, and E. P. Chock, Solid State Commun. **12**, 621 (1973). Note the relation $2J^{(2)} = \Gamma^{(2)}$ between $J^{(2)}$ (Davidov *et al.*) and $\Gamma^{(2)}$ (our paper).

²⁵E. P. Chock, R. Chui, D. Davidov, R. Orbach, D. Shaltiel and L. J. Tao, Phys. Rev. Lett. **27**, 282 (1971).

²⁶S. Oseroff, B. Gehman, S. Schultz, and C. Rettori, Phys. Rev. Lett. **35**, 679 (1975).

²⁷K. R. Lea, M. J. M. Leask, and W. P. Wolf, J. Phys. Chem. Solids **23**, 1381 (1962).

²⁸D. Spånjaard and F. Hartmann-Boutron, J. Phys. (Paris) **30**, 975 (1969).

²⁹See Ref. 15, pp. 275-285.

³⁰See Ref. 15, Eq. (7.9.8).